

The bending behaviour of L-phenylalanine monohydrate soft crystal via reversible hydrogen bonds rupture and remodeling

Yaxiang Gong^{a, ‡}, Yuanfeng Wei^{b, ‡}, Yuan Gao^b, Zungting Pang^b, Jianjun Zhang^{a,*}, Shuai Qian^{b,*}

^a School of Pharmacy, China Pharmaceutical University, Nanjing, 211198, China

^b School of Traditional Chinese Pharmacy, China Pharmaceutical University, Nanjing, 211198, China

[‡]Authors contributed equally.

Corresponding authors:

Dr. Jianjun Zhang

School of Pharmacy, China Pharmaceutical University

Tel.: +86 13951974969, Email address: myamicute@163.com

Dr. Shuai Qian

School of Traditional Chinese Pharmacy, China Pharmaceutical University

Tel.: +86 139 15957175, Email address: silence_qs@163.com

1. Lattice energy determination of L-Phe·H₂O

Method

1.1 Differential scanning calorimetry (DSC)

A differential scanning calorimeter (DSC 250, TA Instruments-Waters, U.S.A.) was used to carry out DSC. Approximately 4 mg of sample (L-Phe·H₂O soft crystal and L-Phe (the raw material, RM)) was placed in a nonhermetic aluminum pan, after which it was heated from 25 to 295 °C at a heating rate of 10 °C/min. The dehydration product of L-Phe·H₂O during the heating process was named as L-Phe form-X. Nitrogen gas was used as the purge gas at 20 mL/min. The data was analyzed by Trios software (version 5.1.1.46572). Each experiment was repeated in triplicate.

1.2 Determination of specific heat capacity of L-Phe form X

A differential scanning calorimetry (DSC 250, TA Instruments-Waters, U.S.A.) was used to determine the specific heat capacity of L-Phe form-X was determined by “three-step” method. The empty aluminum pan, sapphire and sample (4 mg) were heated from 150 to 250 °C with a heating rate of 10 °C /min, respectively. The data was analyzed by Trios software (version 5.1.1.46572). The specific heat capacity of L-Phe form-X in the range of 150~250 °C was recorded.

1.3 Lattice energy calculation of L-Phe·H₂O

The lattice energy of L-Phe·H₂O can be calculated by sublimation enthalpy as follow¹⁻³:

$$E_{\text{lattice}} = -\Delta H_{\text{sub}}(T) - 2RT \quad (1)$$

Where E_{lattice} represents lattice energy, ΔH_{sub} is the sublimation enthalpy determined at a specific temperature (T), R is the gas constant.

Considering the sublimation of crystalline water and proton transfer energy of L-Phe (the energy to be overcome from amphoteric ions to molecules), Eq.(1) should be modified to:

$$E_{\text{lattice}} = -\Delta H_{\text{sub}}(T) - 2RT - p^{\theta}V_1 + \Delta E_{\text{pt}} \quad (2)$$

Where V_1 represents the molar volume of crystalline water at sublimation temperature, p^{θ} represents the standard gas pressure, ΔE_{pt} is the proton transfer energy of amino acids, which is a constant ($-137 \text{ kJ}\cdot\text{mol}^{-1}$).⁴ Besides, according to Charles' law,⁵ V_1 at temperature T_1 can be expressed as:

$$V_1 = V^{\theta}T_1 / T^{\theta} \quad (3)$$

Where T^{θ} represents the Kelvin temperature at 0 °C, $T^{\theta}=273 \text{ K}$, V^{θ} represents the molar volume of ideal gas at 273 K, $V^{\theta}=22.4 \text{ L}$. Thus, making use of Eq (2) and (3), E_{lattice} can be expressed as:

$$E_{\text{lattice}} = -\Delta H_{\text{sub}}(T) - 2RT - p^{\theta} \left(\frac{V^{\theta}T_1}{T^{\theta}} \right) + \Delta E_{\text{pt}} = -\Delta H_{\text{sub}}(T) - 3RT + \Delta E_{\text{pt}} \quad (4)$$

Results

DSC is a common method for determining sublimation enthalpy.^{6,7} The DSC curves of L-Phe·H₂O and L-Phe (RM) were shown in Fig. S1. For L-Phe·H₂O, the endothermic peaks at 127 °C (400 K, $\Delta H_{\text{Dehy}} = 163.2 \pm 2.8 \text{ kJ}\cdot\text{mol}^{-1}$) and 274 °C (547 K, $\Delta H_{\text{fus}} = 64.3 \pm 1.2 \text{ kJ}\cdot\text{mol}^{-1}$) were attributed to dehydration and melting of L-Phe·H₂O, respectively. After dehydration, the specific heat capacity of L-Phe form-X ($C_{\text{p,form-X}}$) was determined to be $197.8 \pm 6.4 \text{ J}\cdot\text{mol}^{-1}\cdot\text{K}^{-1}$. In addition, for L-Phe (RM), only a melting endothermic peak was observed at 274 °C (547K, $\Delta H_{\text{fus}} = 62.1 \pm 1.2 \text{ kJ}\cdot\text{mol}^{-1}$).

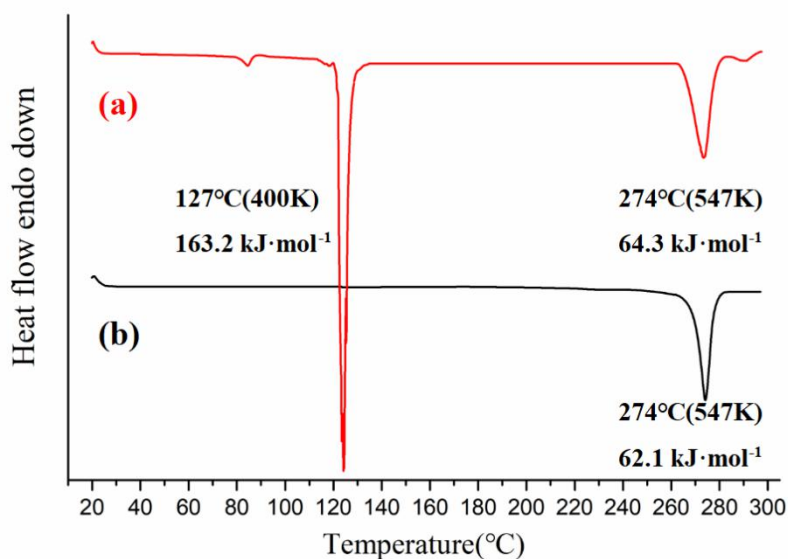
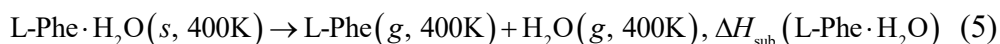
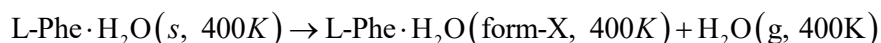


Fig. S1 DSC curves of (a) L-Phe·H₂O and (b) L-Phe (RM).

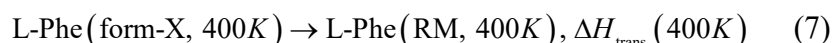
At 400 K, the sublimation reaction of L-Phe·H₂O could be described as follow:



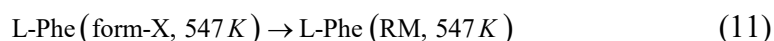
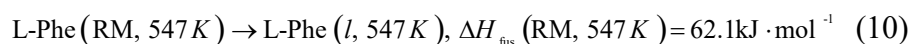
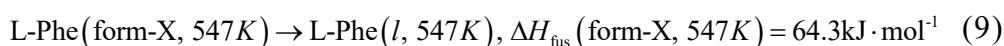
The reaction (5) could be regarded as the sum of Eq. (6), Eq. (7) and Eq. (8):



$$\Delta H_{\text{Dehy}} = 163.2 \pm 2.8 \text{kJ} \cdot \text{mol}^{-1} \quad (6)$$



Eq. (7) could be regarded as the transition from L-Phe form-X to L-Phe RM at 400 K, and the enthalpy change of this process ($\Delta H_{\text{trans}}(400\text{K})$) could be calculated as follow:



$$\Delta H_{\text{trans}}(547K) = \Delta H_{\text{fus}}(\text{form-X}, 547K) - \Delta H_{\text{fus}}(\text{RM}, 547K) = 2.2\text{kJ} \cdot \text{mol}^{-1}$$

$$\Delta H_{\text{trans}}(400K) = \Delta H_{\text{trans}}(547K) + (C_{\text{p,form-X}} - C_{\text{p,RM}})(400K - 547K) = 2.3\text{kJ} \cdot \text{mol}^{-1} \quad (12)$$

Where $C_{\text{p,form-X}}$ and $C_{\text{p,RM}}$ were the specific heat capacity of L-Phe form-X and L-Phe RM. $C_{\text{p,RM}}$ was reported to be $203.1 \pm 1.5 \text{ J} \cdot \text{mol}^{-1} \cdot \text{K}^{-1}$.⁸

Eq. (8) was the sublimation process of L-Phe at 400K, and the enthalpy change of this process ($\Delta H_{\text{sub}}(\text{L-Phe}, 400 \text{ K})$) could be described as follow:

$$\Delta H_{\text{sub}}(\text{RM}, 400K) = \Delta H_{\text{sub}}(\text{RM}, 298K) + \int_{298K}^{400K} (C_{\text{p,g}} - C_{\text{p,RM}})dT = 158.7\text{kJ} \cdot \text{mol}^{-1} \quad (13)$$

Where $C_{\text{p,g}}$ was the specific heat capacity of gaseous L-Phe, $C_{\text{p,g}} = 184 \pm 1 \text{ J} \cdot \text{mol}^{-1} \cdot \text{K}^{-1}$.⁸

Combined with Eq. (6), Eq. (12) and Eq. (13), the sublimation enthalpy of L-Phe·H₂O at 400 K could be described as follow:

$$\begin{aligned} \Delta H_{\text{sub}}(\text{L-Phe} \cdot \text{H}_2\text{O}, 400K) &= \Delta H_{\text{Dehy}}(400K) + \Delta H_{\text{trans}}(400K) + \Delta H_{\text{sub}}(\text{L-Phe}, \text{RM}, 400K) \\ &= (163.2 + 2.3 + 158.7)\text{kJ} \cdot \text{mol}^{-1} = 324.2\text{kJ} \cdot \text{mol}^{-1} \end{aligned}$$

When the calculation result of sublimation enthalpy was substituted into Eq. (4), the lattice energy of L-Phe·H₂O was obtained to be $-112.56 \text{ kcal} \cdot \text{mol}^{-1}$.

2. Crystallographic information for L-Phe·H₂O

Table S1 Crystallographic data of L-Phe·H₂O

Formula	C ₉ H ₁₃ NO ₃
Molecular weight	183.20
Crystal system	monoclinic
Space group	P 2 ₁ (4)
a (Å)	13.0612 (5)
b (Å)	5.4197 (2)
c (Å)	13.8643 (6)
α (°)	90
β (°)	102.611
γ (°)	90
Volume (Å ³)	957.746
Z	Z=4
ρ _{calc} (g/cm ³)	1.271
2θ	2.841 to 50.011
F (000)	392
R ₁	0.0318
wR ₂	0.0825
Goodness-of-fit (GOF)	1.047
Temperature (K)	193 (2)
CCDC No.	2009781

Table S2 The intermolecular hydrogen bond parameters of L-Phe·H₂O

No.	Donor-H...Acceptor	D-A/ Å	H...A/ Å	D-H...A/ °
1	O6-H6B(H ₂ O)...O1(L-Phe)	0.846	1.830	9.634
2	N1-H1A(L-Phe)...O6(H ₂ O)	0.910	1.849	176.645
3	O5-H5B(H ₂ O)...O4(L-Phe)	0.874	1.984	149.043
4	N2-H2A(L-Phe)...O4(L-Phe)	0.910	2.020	78.701
5	N2-H2B(L-Phe)...O3(L-Phe)	0.910	1.878	173.345
6	N1-H1C(L-Phe)...O3(L-Phe)	0.910	2.070	139.319
7	N1-H1C(L-Phe)...O2(L-Phe)	0.910	2.388	97.980
8	N2-H2C(L-Phe)...O2(L-Phe)	0.910	1.965	152.045
9	N2-H2C(L-Phe)...O3(L-Phe)	0.910	2.412	110.203

3. Analysis the bending region by *in situ* micro-infrared and *in situ* micro-Raman

Table S3 Micro-infrared assignments for L-Phe·H₂O

Wavenumber (cm ⁻¹) in straight state	Wavenumber (cm ⁻¹) in bent state	Wavenumber difference (cm ⁻¹)	Assignments
3358 ± 0.23	3363 ± 0.43	5	O-H str.
3028 ± 0.44	3062 ± 0.57	34	NH₃⁺ asym. str.
2846 ± 0.40	2846 ± 0.29	0	C-H str.
1598 ± 0.48	1560 ± 0.51	38	NH₃⁺ asym.bending and COO⁻ asym. str.
1508 ± 0.40	1500 ± 0.32	8	NH₃⁺ sym.bending
1404 ± 0.17	1417 ± 0.22	13	COO⁻ asym. str.
1311 ± 0.13	1311 ± 0.49	0	CH ₂ wagging
1197 ± 0.38	1200 ± 0.43	3	C-CH bending
1148 ± 0.22	1150 ± 0.76	2	CH ₂ twisting
1041 ± 0.67	1038 ± 0.91	3	C-C str.
980 ± 0.53	979 ± 0.43	1	CH ₂ rocking
915 ± 0.31	918 ± 0.35	3	C-CH bending
857 ± 0.88	859 ± 0.64	2	C-H out-of plane deformation
779 ± 0.65	782 ± 0.82	3	C-C skeletal str.
694 ± 0.50	695 ± 0.46	1	C-H out-of plane deformation
516 ± 0.66	521 ± 0.19	5	C-COO⁻ deformation

Table S4 Micro-Raman assignments for L-Phe·H₂O

Wavenumber (cm ⁻¹) in straight state	Wavenumber (cm ⁻¹) in bent state	Wavenumber difference (cm ⁻¹)	Assignments
138 ± 0.50	146 ± 0.38	8	Lattice modes
251 ± 0.57	269 ± 0.55	18	Lattice modes
346 ± 0.78	347 ± 0.60	1	C-C-C-C in phase vibration
426 ± 0.41	432 ± 0.50	6	COO⁻ rocking
497 ± 0.60	489 ± 0.43	9	H₂O
541 ± 0.34	539 ± 0.22	2	C ₆ H ₅ -C in plane deformation
618 ± 0.69	624 ± 0.78	6	COO⁻ rocking
823 ± 0.46	822 ± 0.61	1	CH ₂ rocking
846 ± 0.50	853 ± 0.74	7	NH₃⁺ deformation
1006 ± 0.37	1004 ± 0.50	2	C-C of the benzene ring sym. str
1169 ± 0.65	1177 ± 0.27	8	C-N str.
1194 ± 0.56	1186 ± 0.84	8	NH₃⁺ rocking
1310 ± 0.94	1311 ± 0.59	1	CH ₂ rocking
1416 ± 0.30	1422 ± 0.47	6	COO⁻ sym. str
1498 ± 0.29	1506 ± 0.35	8	NH₃⁺ sym. str
1587 ± 0.86	1588 ± 0.53	1	C-C ring sym. str of the benzene
1607 ± 0.73	1607 ± 0.84	0	C-C ring sym. str of the benzene

4. Difference between the calculated lattice energy and experimental value

Table S5 Lattice energies of L-Phe·H₂O using different combination of force fields and charge assignment rules

Force field/Charge rule	Calculated values (kcal/mol)	Experimental values (kcal/mol)	The difference between experimental and calculated values (kcal/mol)
COMPASS/Forcefield assigned	-29.683		-82.877
COMPASS/Gasteiger	-102.121		-10.439
COMPASS/Qeq	-55.048		-57.512
CVFF/Forcefield assigned	-29.421		-83.139
CVFF/Qeq	-51.438		-61.122
CVFF/Gasteiger	-95.941	-112.56	-16.619
Universal/Qeq	-73.995		-38.565
Universal/Gasteiger	-58.001		-54.559
Dreiding/Gasteiger	-115.105		2.545
Dreiding/Qeq	-66.901		-45.659
PCFF/Forcefield assigned	-26.730		-85.83
PCFF/Gasteiger	-95.941		-16.619
PCFF/Qeq	-56.484		56.076

5. Attachment energy calculation

Table S6 Attachment energies and molecular interaction energies in each direction of L-Phe·H₂O soft crystal

h k l	$E_{att}(\text{Total})$	$E_{att}(\text{vdW})$	$E_{att}(\text{Electrostatic})$	$E_{att}(\text{H-bond})$
[0 1 0]	-76.858 kcal/mol	-4.187 kcal/mol	-62.447 kcal/mol	-10.223 kcal/mol
[1 0 0]	-18.078 kcal/mol	-2.26 kcal/mol	-14.187 kcal/mol	-1.627 kcal/mol
[0 1 1]	-65.453 kcal/mol	-3.061 kcal/mol	-55.276 kcal/mol	-7.117 kcal/mol
[1 1 0]	-68.153 kcal/mol	-2.960 kcal/mol	-57.103 kcal/mol	-8.089 kcal/mol

References

1. C. Ouvrard and J. B. Mitchell, *Acta Crystallographica Section B: Structural Science*, 2003, **59**, 676-685.
2. M. Salahinejad, T. C. Le and D. A. Winkler, *Journal of chemical information and modeling*, 2013, **53**, 223-229.
3. A. Hagler, E. Huler and S. Lifson, *Journal of the American Chemical Society*, 1974, **96**, 5319-5327.
4. V. Biskar-Leib and M. F. Doherty, *Crystal Growth & Design*, 2015, **3**, 221-237.
5. G. Chandan and M. Cascella, 2019.
6. J. P. Murray and J. O. Hill, *Thermochimica Acta*, 1984, **72**, 341-347.
7. A. Rojas-Aguilar, E. Orozco-Guare?O, Mart?, M. Amp, #x and nez-Herrera, *Journal of Chemical Thermodynamics*, 2001, **33**, 1405-1418.
8. V. V. Tyunina, A. V. Krasnov, E. Y. Tyunina, V. G. Badelin and G. V. Girichev, *Journal of Chemical Thermodynamics*, 2014, **74**, 221-226.